LASER PHASE NOISE MEASUREMENTS AND ANALYSIS IN A HIGH-POWER OPTICAL ENHANCEMENT CAVITY

Z. Yang*[1], Y. Zhao[1], Y. Huang[1], X. Liu†[1], X. Lu[1], Q. Tian[1], W. Huang[1],
C. Tang[1], L. Yan‡[1], A. Renaux[2,3,4], R. Chiche[2,3,4], K. Dupraz[2,3,4], A. Martens[2,3,4], F. Zomer[2,3,4]
[1]Department of Engineering Physics, Tsinghua University, Beijing, China
[2]Université Paris-Saclay, Orsay, France
[3]CNRS/IN2P3, Paris, France
[4]IJCLab, Orsay, France

Abstract

Optical resonators serve as excellent spatiotemporal filters and are widely used for stabilizing laser frequency. They can also function as passive optical enhancement cavities (OECs), providing power gains of thousands to tens of thousands. High-power OECs hold promise for applications such as steady-state microbunching (SSMB) advanced light sources and laser interferometer gravitational-wave observatory (LIGO). However, systematic studies on the phase noise characteristics of high-power OECs remain lacking. In this paper, based on a high-power OEC platform, we measure the phase noise of both the injected laser and the transmitted laser, and investigate the influence of key cavity-locking parameters on the phase noise performance, thereby providing valuable references for the application of high-power OECs.

INTRODUCTION

Optical resonators, leveraging coherent superposition of light fields, enable resonant enhancement of laser power while simultaneously acting as spatiotemporal filters for optical fields. The intracavity field exhibits excellent transverse mode quality and frequency stability, leading to a wide range of applications. Carefully designed ultrastable cavities can be used as optical frequency references, achieving laser outputs with ultra-low linewidths [1, 2]. The phase-sensitive characteristic of optical cavities has also been exploited in laser interferometer gravitational-wave observatory (LIGO) [3]. Moreover, advances in coating techniques for ultrahigh-reflectivity mirrors have facilitated the development of optical enhancement cavities (OECs), where power gains of more than ten thousand can produce megawatt-level intracavity circulating power [4–6]. Such high-power cavities offer new potential solutions for fields such as inertial confinement fusion and ion neutralization [7, 8]. OECs are also widely used in accelerator-based advanced light source research, for example, in the ThomX project, the Gamma Factory, and the steady-state microbunching (SSMB) advanced light source [4, 5, 9–11]. Current research on high-power OECs has focused primarily on stored intracavity power, mirror thermal effects, and damage thresholds [4–6], with few studies addressing the phase noise characteristics of high-power OECs. Nevertheless, phase noise performance is critically important for applications such as SSMB and LIGO [3, 11, 12]. Taking SSMB as an example, it not only requires megawatt-level intracavity power but also stable phase locking among several high-power cavities, which imposes stringent demands on cavity design. Based on a megawatt-level OEC platform, we employ the heterodyne self-beat technique to measure the phase noise properties of both the injected laser and the transmitted laser. We analyze the possible underlying mechanisms and compare the influence of different cavity-locking parameters on phase noise performance, thereby providing a new perspective for cavity optimization.

* yang-z23@mails.tsinghua.edu.cn
† liuxing09thu@gmail.com
‡ yanlx@mail.tsinghua.edu.cn

EXPERIMENTAL SETUP AND MEASUREMENT METHOD

We have constructed a four-mirror OEC platform consisting of high-reflectivity mirrors, a vacuum system, a low-noise continuous-wave laser, an optical transmission line, and a cavity locking electronics system, as shown in Fig. 1. The cavity itself is composed of four high-reflectivity mirrors: two flat mirrors (M1, M2) and two concave mirrors (M3, M4), where M1 serves as the input coupling mirror. Due to minor contamination from environmental dust and imperfections in coating smoothness, the experimentally measured finesse of the cavity is 26,000, lower than the theoretical value of 32,000, corresponding to an actual cavity linewidth of approximately 3.1 kHz. The low-noise continuous-wave laser can deliver an incident laser power of up to approximately 130 W. The optical transmission line consists of lenses, waveplates, and motorized mirrors, enabling mode matching, polarization matching, and alignment of the incident laser to the cavity resonance mode. The Pound-Drever-Hall (PDH) locking technique is utilized to lock the laser frequency to the cavity resonance. It features a dual-loop structure: a digital slow loop using a piezoelectric transducer (PZT) as the actuator and an analog fast loop using an acousto-optic modulator (AOM) as the actuator. Based on this platform, we measured the phase noise of both the injected laser and the transmitted laser using a heterodyne self-beat technique, as illustrated in Fig. 1. The laser under test was coupled into an optical fiber and split into two paths. One path was frequency-shifted by 110 MHz using an AOM, while the other path propagated through a 1 km

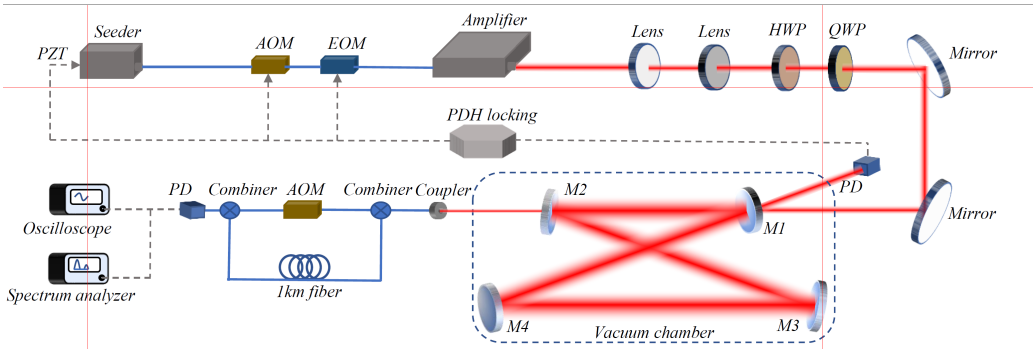

Figure 1: Layout of the high-power OEC and the method for phase noise measurement.

delay fiber to ensure loss of mutual coherence. The phase noise was then obtained by demodulating the beat signal between the two paths. The measurements of the injected and transmitted lasers differ only in the probing location: before and after the optical cavity, respectively.

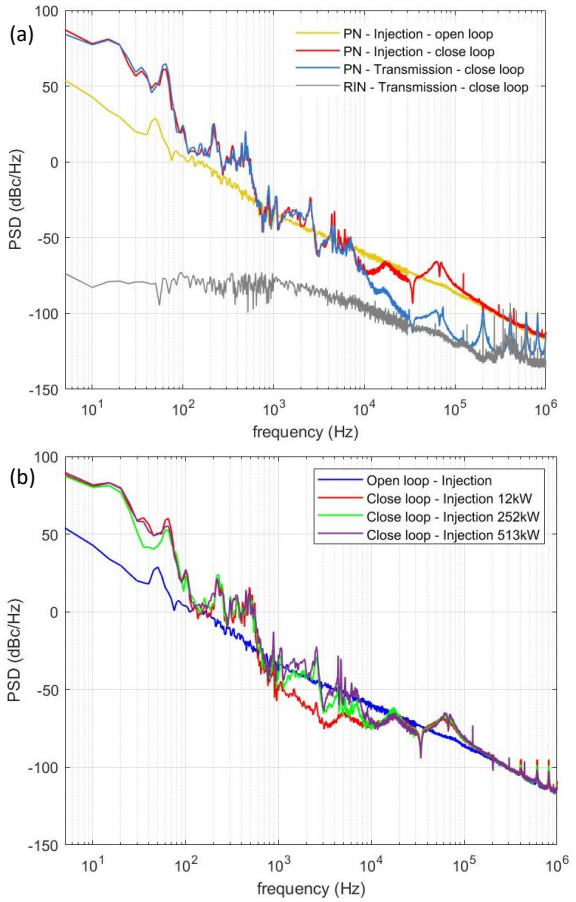

Figure 2: (a) The phase noise (PN) PSD of the injected laser under open-loop and closed-loop conditions, and the phase noise PSD and RIN of transmitted laser from the cavity under closed-loop. (b) The phase noise PSD of the injected laser at different intracavity powers.

MEASUREMENT RESULTS AND ANALYSIS OF PHASE NOISE

Phase-noise measurements were conducted for the injected laser in both the open-loop and closed-loop states, as well as for the transmitted laser in the closed-loop state. The corresponding phase-noise power spectral densities (PSDs) are shown in Fig. 2(a). Testing phase noise in open-loop state is actually testing the noise of the laser itself, determined by the intrinsic oscillator noise and amplifier-induced fluctuations, resulting in an integrated root-mean-square (RMS) frequency jitter of 7.3 kHz over 10 Hz-1 MHz. When locked, the cavity operates at 500 kW intracavity power. The laser frequency is constrained to the cavity resonance, and the phase-noise spectrum is shaped by both the servo dynamics and the cavity response. Notably, a pronounced increase in phase noise is observed in the low-frequency range [5 Hz, 1 kHz]. As shown in Fig. 2(b), when the intracavity powers are 12 kW, 252 kW, and 513 kW, the phase noise of the injected laser exhibits good consistency in the low-frequency range below 1 kHz. Consequently, cavity thermal noise is unlikely to be the dominant contributor to the observed low-frequency phase noise. Instead, mechanical vibrations of the cavity structure and electronic noise from the locking loop are the primary sources. This result can be expected, as the current cavity design incorporates no active measures to stabilize the cavity length. From a few kilohertz to 1 MHz, the phase noise of the transmitted laser is substantially lower than that of both the injected laser and the free-running laser, confirming that the optical cavity maintains a high finesse under high-power operation and exhibits an intrinsic low-pass filtering effect. Over the frequency range [1 kHz, 1 MHz], the RMS frequency jitters are 2.60 kHz for the transmitted laser and 6.16 kHz for the injected laser under closed-loop conditions. In addition, a prominent servo bump appears at 65 kHz in the phase noise PSD of the injected laser, originating from the limited bandwidth of the feedback loop [2]. The distinct resonant peaks at 203.4 kHz and its harmonics are introduced by the self-heterodyne technique, with their specific frequencies determined by the length of the delay fiber. The relative intensity noise (RIN) of the transmitted laser, shown as the gray curve in Fig. 2(a), exhibits a cutoff frequency consistent with the measured cavity linewidth, further confirming that the finesse is preserved at

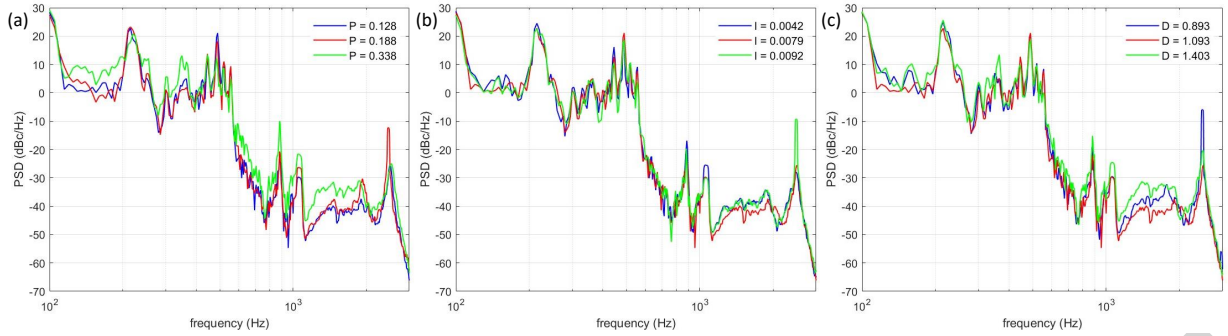

Figure 3: Phase noise PSD of the transmitted laser under different PID parameters. Since the phase noise exhibits almost no variation below 100 Hz and above 3 kHz, these frequency ranges are not shown in the figure.

high average power. As shown in Fig. 2(b), the correlation between the phase noise of the injected laser and the intracavity power is mainly observed in the frequency range of 1 kHz to 10 kHz, with a trend that higher intracavity power leads to higher phase noise PSD. Therefore, the phase noise in this frequency range may be attributed to thermal effects of the optical cavity, such as coating thermal noise [13]. Meanwhile, our experiments also reveal that the parameter settings of the cavity locking loop significantly affect the phase noise in this frequency band. The proportional-integral-derivative (PID) parameters of the slow loop and the frequency modulation parameters of the AOM in the fast loop serve as the main control variables. Under a fixed intracavity power of approximately 250 kW, we measured the phase noise of the transmitted laser for different sets of loop control parameters. The influence of each parameter was investigated using a single-variable control method. The measurement results are presented in Fig. 3. It is evident that the P and D parameters have a more significant impact on phase noise than the I parameter. This is because the P and D settings are designed to provide fast response to frequency noise, whereas the I parameter primarily eliminates static errors and mainly affects low-frequency noise performance. The AOM serves as the actuator of the analog fast loop to rapidly compensate for high-frequency frequency noise of the laser. Specifically, the error signal generated by the PDH method is used as the external modulation signal for a signal generator operating in frequency modulation (FM) mode, which then outputs an electrical signal (center frequency 110 MHz) whose frequency deviation is proportional to the amplitude of the error signal. The proportionality coefficient is defined as the frequency deviation (FM dev). This signal is amplified and drives the AOM, thereby compensating for frequency fluctuations of the injected laser. The FM dev acts as a tunable gain of the fast loop and significantly affects the phase noise performance (Fig. 4). In the frequency range of 1 kHz to 10 kHz, the phase noise PSD reaches its minimum when the FM dev is set to 900 kHz, indicating that the loop achieves the efficient suppression of phase noise in this band under this setting. It should be noted that the optimal choice of AOM parameters is jointly determined by factors such as the loop architecture, signal delay, and the frequency noise characteristics of the laser. Furthermore, because the AOM is primarily used to suppress high-frequency noise, its parameters play a crucial role in determining the overall loop bandwidth. A larger FM dev results in a higher loop bandwidth, which shifts the servo bump to a higher frequency. At the same time, the phase margin is reduced, making the servo bump more pronounced.

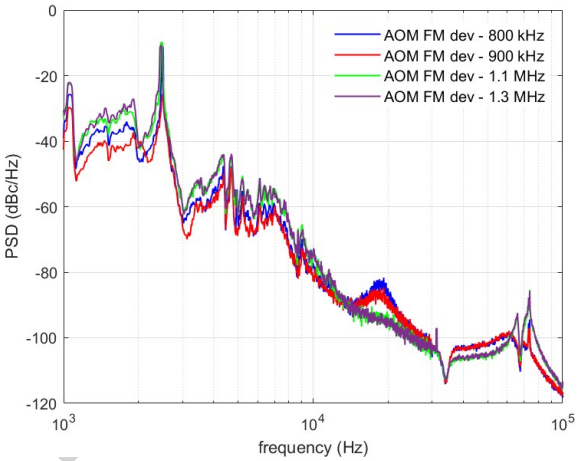

Figure 4: Phase noise of the transmitted laser under different AOM FM deviation settings.

CONCLUSION

This paper presents phase noise measurement results obtained on the high-power OEC platform at Tsinghua University. Due to mechanical vibrations of the cavity structure and electronic noise of the feedback loop, the low-frequency phase noise increases significantly compared with that of the seed laser. Above 10 kHz, the phase noise of the transmitted laser under closed-loop operation is substantially lower than that of the injected laser, demonstrating the low-pass filtering effect of the cavity. Apart from the cavity itself, the parameters of the cavity locking loop also strongly influence the phase noise performance. The phase noise characteristics exhibited by the high-power OECs provide a valuable reference for their applications and offer a new perspective for optimizing cavity design and achieving more stable locking.

ACKNOWLEDGMENTS

This work was funded by the National Key Research and Development Program of China (Grant No. 2022YFA1603403), the Beijing Outstanding Young Scientist Program (No. JWZQ20240101006), and the National Natural Science Foundation of China (NSFC Grants No. 12405181).

REFERENCES

[1] T. Kessler *et al.*, "A sub-40-mHz-linewidth laser based on a silicon single-crystal optical cavity", *Nat. Photonics*, vol. 6, no. 10, pp. 687–692, 2012. doi:10.1038/nphoton.2012.217

[2] Y.-X. Chao, Z.-X. Hua, X.-H. Liang, Z.-P. Yue, L. You, and M. K. Tey, "Pound–drever–hall feedforward: laser phase noise suppression beyond feedback", *Optica*, vol. 11, no. 7, pp. 945–953, 2024. doi:10.1364/OPTICA.516838

[3] E. Capote *et al.*, "Advanced LIGO detector performance in the fourth observing run", *Phys. Rev. D*, vol. 111, no. 6, p. 062002, 2025. doi:10.1103/PhysRevD.111.062002

[4] X.-Y. Lu *et al.*, "710 kW stable average power in a 45,000 finesse two-mirror optical cavity", *Opt. Lett.*, vol. 49, no. 23, pp. 6884–6887, 2024. doi:10.1364/OL.543388

[5] X.-Y. Lu *et al.*, "Stable 500 kW average power of infrared light in a finesse 35,000 enhancement cavity", *Appl. Phys. Lett.*, vol. 124, no. 25, p. 251105, 2024. doi:10.1063/5.0213842

[6] X. Liu *et al.*, "Continuous-wave optical enhancement cavity with 30-kW average power", *Chin. Phys. B*, vol. 32, no. 3, p. 034206, 2023. doi:10.1088/1674-1056/ac873e

[7] M. Q. Tran *et al.*, "Status and future development of heating and current drive for the EU DEMO", *Fusion Eng. Des.*, vol. 180, p. 113159, 2022. doi:10.1016/j.fusengdes.2022.113159

[8] A. Simonin *et al.*, "Negative ion source development for a photoneutralization based neutral beam system for future fusion reactors", *New J. Phys.*, vol. 18, no. 12, p. 125005, 2016. doi:10.1088/1367-2630/18/12/125005

[9] M. Alkadi *et al.*, "Commissioning of ThomX compton source subsystems and demonstration of 10^{10} x-rays/s", *Phys. Rev. Accel. Beams*, vol. 28, no. 2, p. 023401, 2025. doi:10.1103/PhysRevAccelBeams.28.023401

[10] A. Martens *et al.*, "Design of the optical system for the gamma factory proof of principle experiment at the CERN Super Proton Synchrotron", *Phys. Rev. Accel. Beams*, vol. 25, no. 10, p. 101601, 2022. doi:10.1103/PhysRevAccelBeams.25.101601

[11] X. Deng *et al.*, "Experimental demonstration of the mechanism of steady-state microbunching", *Nature*, vol. 590, no. 7847, pp. 576–579, 2021. doi:10.1038/s41586-021-03203-0

[12] Z. Li, X. Deng, Z. Pan, C. Tang, and A. Chao, "Generalized longitudinal strong focusing in a steady-state microbunching storage ring", *Phys. Rev. Accel. Beams*, vol. 26, no. 11, p. 110701, 2023. doi:10.1103/PhysRevAccelBeams.26.110701

[13] A. Gurkovsky and S. Vyatchanin, "The thermal noise in multilayer coating", *Phys. Lett. A*, vol. 374, no. 33, pp. 3267–3274, 2010. doi:10.1016/j.physleta.2010.06.012